Cécile Raillard*, Audrey Maudhuit, Valérie Héquet, Laurence Le Coq, Jean Sablayrolles, and Laurent Molins

# Use of Experimental Designs to Establish a Kinetic Law for a Gas Phase Photocatalytic Process

**Abstract:** The photocatalytic degradation of three common indoor VOCs – acetone, toluene and heptane – is investigated in a dynamic photocatalytic oxidation loop using Box–Behnken designs of experiments. Thanks to the experimental results and the establishment of a kinetic rate law based on a simplified mechanism, a predictive model for the VOC degradation involving independent factors is developed. The parameters under investigation are initial concentration, light intensity and air velocity through the photocatalytic medium. The obtained model fits properly the experimental curves in the range of concentration, light intensity and air flow studied.

**Keywords:** photocatalytic oxidation, experimental designs, kinetic rate law

***Corresponding author: Cécile Raillard,** L'UNAM, GEPEA, UMR CNRS 6144, Ecole des Mines de Nantes, Nantes, France, E-mail: Cecile.Raillard@univ-nantes.fr
**Audrey Maudhuit:** E-mail: audrey.maudhuit@phytosynthese.com, **Valérie Héquet:** E-mail: Valerie.Hequet@mines-nantes.fr, **Laurence Le Coq:** E-mail: Laurence.Le-Coq@mines-nantes.fr, L'UNAM, GEPEA, UMR CNRS 6144, Ecole des Mines de Nantes, Nantes, France
**Jean Sablayrolles,** Saint Gobain Recherche, Aubervilliers, France, E-mail: Jean.Sablayrolles@saint-gobain.com
**Laurent Molins,** Saint-Gobain Quartz, Nemours, France, E-mail: Laurent.Molins@saint-gobain.com

## 1 Introduction

Indoor air quality has been of major interest for more than three decades, because indoor air pollutants impact human health, comfort and productivity. Volatile organic compounds (VOCs) are recognized as being among the most abundant chemical pollutants in the indoor air that people breathe during at least 80% of their daily lives. VOCs are emitted from many building materials, furnishings and household products and have been documented as sources of reactive compounds and reaction products. A hundred different species of VOCs can be found in indoor air. Although the concentration of each of them is below 100 parts per billion, the total concentration of VOCs reaches about one part per million (ppm). Such compounds can be quickly and economically removed from indoor air by many advanced technologies, including photocatalytic oxidation (PCO). PCO is an innovative and promising approach which appears well adapted to the specificities of indoor air pollution [1–4]. However, the development of photocatalysis for indoor air treatment will only be possible if kinetic laws allowing the scaling up of the process in real conditions are available [5]. This work presents a methodology to answer this specific point. The chart in Figure 1 gives an overview of the methodology applied.

Few reports deal with the application of the statistical design of experiments (DOE) to the PCO process [6]. Most studies dealing with kinetics make use of the traditional one-factor-at-a-time (OFAT) approach. If the factors involved in the process are independent, the most common practice is the OFAT while holding all other parameters constant. However, not only are factors rarely independent, but the OFAT approach is also time-consuming. Response surface methodology based on statistical DOE appears to be more appropriate since it accounts for interaction effects between the studied variables. Hence, the originality of the methodology applied in this work rests on the fact that the DOE was used both to optimize the process and to model the reaction kinetics. To implement the DOE in such works, the first step consists of screening factors in order to select those that may play a significant role, according to the specific application of the process. This can be done using the very well-documented literature on the photocatalytic process for air treatment. The efficiency of the photocatalytic reaction in the gas phase may be affected by several variables including the initial concentration of target compounds, UV wavelength and light intensity, catalyst dose and/or characteristics, temperature, relative humidity and air flow [7]. In the present work, the photocatalytic medium is an industrial commercialized one so that the characteristics and the quantity of the catalyst are imposed. Concerning the temperature, Hermann reported that photocatalytic activity is very little

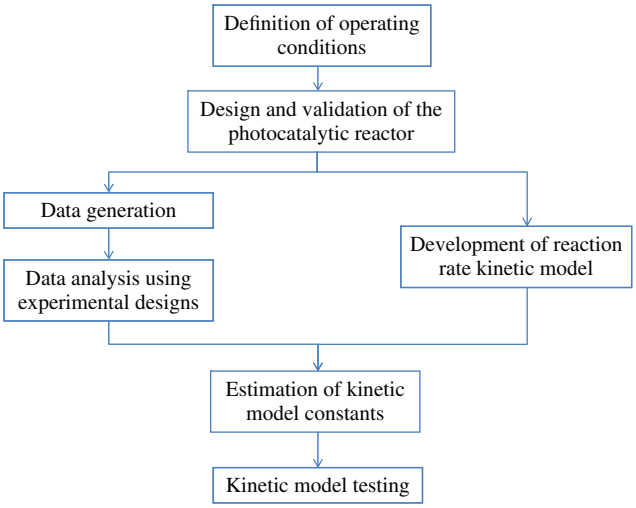


**Figure 1** Flowchart of the methodological approach

impacted in the range 20–80°C [7]. In indoor environments, such as homes and administrative buildings, the temperature is generally between 18 and 26°C [8]. Thus, temperature was not considered very relevant and was fixed at 24°C. Relative humidity is related to the quantity of water vapour in the air, which can have two antagonistic effects on the photocatalytic reaction. According to the level of relative humidity at a fixed temperature, the reaction kinetic rate is either increased or decreased [3, 9, 10]. In indoor environments, and particularly in French ones, the relative humidity is generally between 40 and 60% and is quite well controlled so that this factor can be considered constant. Hence, in the present work, this variable was not included in the DOE. For UV wavelength, different conclusions have been reported in the literature. Mohseni and David [11] obtained similar degradation rates for the PCO of vinyl chloride, whatever was the UV wavelength (254 and 365 nm). On the contrary, Shie et al. [12] showed that the oxidation rate of formaldehyde was 25% higher with UVA (365 nm) than with UVC (254 nm). In this paper, only those results obtained with UVA are presented even though the impact of UV wavelength was also studied. The other parameters cited above were taken into account in this study by implementing the Box–Behnken design (BBD) technique.

The objective of this study is thus to optimize the photocatalytic degradation of three common indoor VOCs – acetone, toluene and heptane – using BBDs of experiments and to develop a predictive model for the VOC degradation rate involving independent factors. The parameters under investigation are initial concentration, light intensity and air velocity through the photocatalytic medium.

# 2 Materials and methods

## 2.1 Photocatalytic medium

A commercial $TiO_2$-catalyst constituted of non-woven quartz fibres linked by a patented technology was used in this study (patent # WO03010106). It is composed of titanium dioxide powder (16 g $m^2$) linked on the quartz fibre support by an inorganic binder whose details cannot be given for industrial reasons.

The specific surface area of this photocatalyst is above 100 $m^2\ g^{-1}$. It develops a majority of pores with diameters less than 50 nm, and the porous volume is equal to 0.075 $cm^3\ g^{-1}$ of photocatalytic medium. In the kinetic study, the photocatalyst was used as a filter perpendicular to the air flow. Experiments were performed on the photocatalyst to investigate the hydrodynamic behaviour of a single layer. A linear laminar regime governed by Darcy's law was observed. Pressure drops were measured for an upstream flow rate of up to 150 $m^3\ h^{-1}$, corresponding to Reynolds numbers from 1,200 to 6,300. The generated pressure drops were low and well adapted for the targeted application (Figure 2).

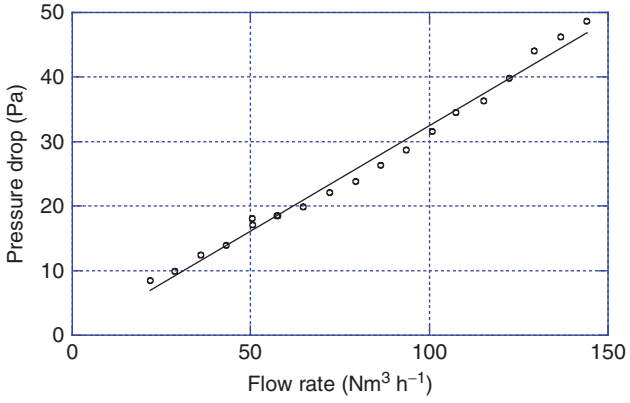


**Figure 2** Generated pressure drops versus the upstream flow rate

## 2.2 Dynamic photocatalytic pilot

A 420-L dynamic photocatalytic pilot was specially designed and constructed as described in previous articles [13, 14]. The geometry of the device is presented in Figure 3.

It was optimized in order to ensure a homogeneous flow field thanks to CFD simulation, photon flux and concentration over the whole photocatalyst surface (Figure 4).

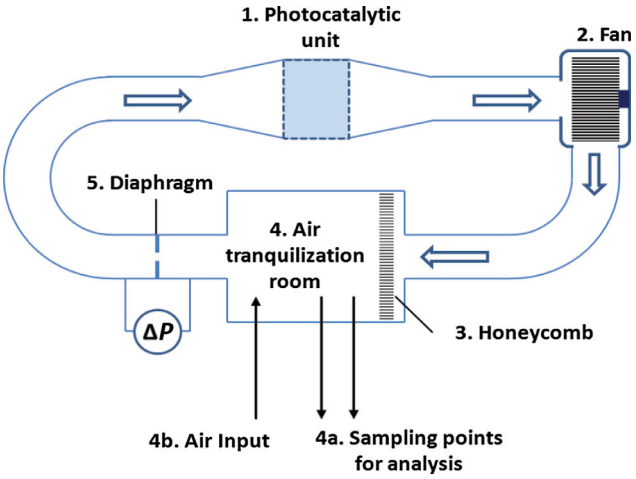


**Figure 3** Geometry of the dynamic photocatalytic reactor: (1) photocatalytic unit containing the $TiO_2$ photocatalytic medium and the UV lamps, (2) fan, (3) honeycomb, (4) air tranquilization chamber, (4a) sampling points, (4b) air input and (5) diaphragm

The distance between the four UV lamps (PL-S, 9 W, Philips, 365 nm) and the photocatalytic medium was adjusted in order to provide a maximum light irradiation of 4 mW $cm^{-2}$. The flow rate during the experiments ranged from 30 to 150 $m^3$ $h^{-1}$. The procedure for collecting data using this photocatalytic reactor is described elsewhere [14]. Initial concentrations of acetone, toluene and heptane ranged from 5 to 50 ppm. The VOC and carbon dioxide concentrations were followed using a gas chromatograph (MTI Analytical Instruments, M200) with a flame ionization detector and a catharometer, respectively.

## 2.3 DOE methodology

For the photocatalytic process, as mentioned in Section 1, three main parameters were identified as potentially influencing VOC photocatalytic degradation: light intensity $I$, initial concentration $C_0$ and upstream air velocity $v$. Consequently, a three-factor three-level BBD with three central points was used for each pollutant taken into account. Three main BBDs were then conducted in the present study. BBDs are a class of rotatable or nearly rotatable second-order designs based on three-level incomplete factorial designs [15]. For three factors, the graphical representation can be seen as a cube that consists of the central point and the middle points of the edges. The number of experiments ($N$) required for the development of a BBD is defined as $N = 2k(k-1) + C_p$ where $k$ is the number of factors and $C_p$ is the number of central points. The method consists of defining a minimum or low level (coded −1), a central or medium level (coded 0) and a high or maximum level (coded +1) for each experimental factor. The experiments were carried out under the conditions defined in Table 1 with light intensity $I$ ranging from 1 mW $cm^{-2}$ (code −1) to 4 mW $cm^{-2}$ (code +1), initial concentration $C_0$ ranging from 5 ppm (code −1) to 50 ppm (code +1) and upstream air velocity $v$ ranging from 0.2 m $s^{-1}$ (code −1) to 1 m $s^{-1}$ (code +1).

The experimental error was assessed by carrying out the experiment for the central point (0,0,0) of the DOE in triplicate.

Two different responses $y$ were used to analyse BBD results: the initial reaction rate $r_0$, principally to study the

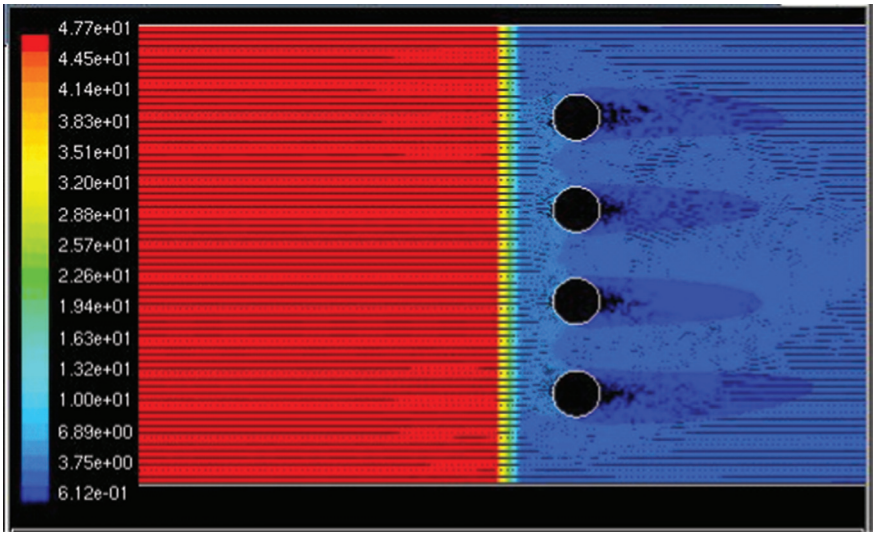


**Figure 4** Velocity stream lines and pressure field in the reactor

**Table 1** Design matrix with coded factor levels

| Experiment number | $I$ | $C_0$ | $v$ |
|---|---|---|---|
| 1 | 0 | 0 | 0 |
| 2 | 0 | 0 | 0 |
| 3 | 0 | 0 | 0 |
| 4 | 0 | +1 | −1 |
| 5 | 0 | −1 | +1 |
| 6 | 0 | −1 | −1 |
| 7 | 0 | +1 | +1 |
| 8 | +1 | 0 | +1 |
| 9 | +1 | +1 | 0 |
| 10 | +1 | −1 | 0 |
| 11 | +1 | 0 | −1 |
| 12 | −1 | 0 | −1 |
| 13 | −1 | −1 | 0 |
| 14 | −1 | +1 | 0 |
| 15 | −1 | 0 | +1 |

effects of factors, and the conversion rate after 60 min of reaction, mainly for synthesizing the kinetic model. A quadratic model described by eq. (1) was evaluated for the experimental responses.

$$y = b_0 + b_1 C_0 + b_2 I + b_3 v + b_{11} C_0^2 + b_{22} I^2 + b_{33} v^2 + b_{12} C_0 I + b_{13} C_0 v + b_{23} I v \quad (1)$$

where $C_0$ is the initial concentration of pollutant, $I$ the light intensity, $v$ the upstream air velocity, and $b_i$ and $b_{ij}$ ($i = 0$ to 3, $j = 1$–3) are constants determined for each surface of response. A Student test was also performed for each DOE in order to identify which factors and interactions in the proposed quadratic model are significant with 95% confidence.

# 3 Results and discussion

## 3.1 Photocatalytic degradation of the three pollutants

A dimensionless study of the experimental degradation curves was carried out to make their comparison easier. The degradation half-life time $t^*$ and the initial concentration $C_0$ for each experiment were used to plot the dimensionless curves. The objective of this part of the work was to make sure that all degradation kinetics for the three pollutants follow the same trend and can be analysed in the same way. Looking at Figure 5 in which three dimensionless curves of toluene degradation are represented for different operating conditions, it appears that the three curves are merged together. Furthermore, the dimensionless curves can be divided into three areas: first a decrease in the concentration following a power relation for a ratio $C/C_0$ up to 0.45 is observed, then there is an area of transition until the ratio $C/C_0$ reaches about 0.7 and finally, in the last zone, a linear decrease in the concentration occurs. A similar study was conducted for the two other pollutants, acetone and heptane, and showed the same trend. It was thus concluded that transfer and reaction mechanisms are equivalent for the three

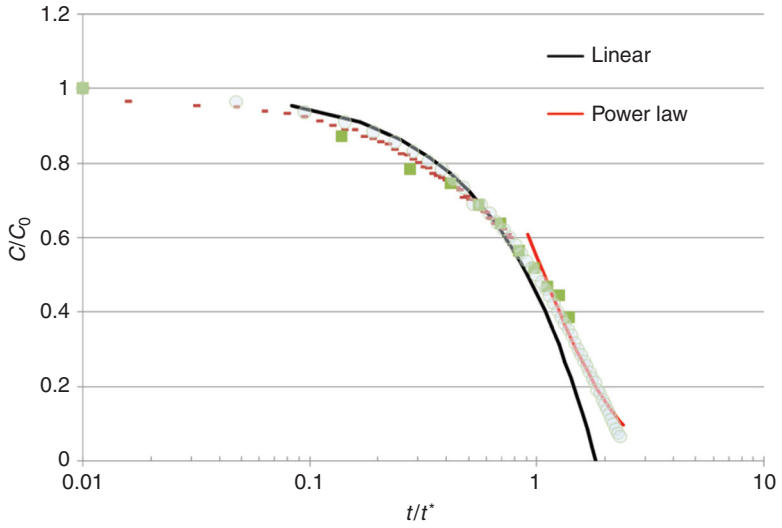


**Figure 5** Examples of dimensionless curves for toluene degradation under different operating conditions

studied compounds and for the implemented range of concentrations, light intensities and upstream air velocities.

## 3.2 DOE analysis and effects of factors and interactions on the initial reaction rate

The Box–Behnken experimental design enables the influence of each studied factor on the observed responses (initial reaction rate and conversion yield) to be quantified. In the following part, the roles of each factor, as well as their interactions, are discussed looking at the behaviour of the initial reaction rate $r_0$. With this objective, surfaces of responses and cross-sections are plotted in order to visualize properly the evolution of $r_0$ with $C_0$, $I$ and $v$. Table 2 indicates the $p$ values on the $b_{ij}$ coefficients of eq. (1) calculated by the Student test ($t$-test) considering the reaction rate as the DOE response.

For the other responses (conversion yields), factors for which the coefficient in the quadratic model were significant according to the Student test were the same as for the initial reaction rate. Due to these results, attention is mainly focused on the influence of initial concentration $C_0$ and light intensity $I$ in the following paragraphs. The influence of upstream velocity $v$ is also considered as its role is interesting in terms of mass transfer although this factor was not identified as significant in the $t$-test. Interactions between factors are not discussed hereafter.

**Table 2** $p$ values on the coefficients in the quadratic model for $r_0$ as the DOE response

| $b_i$ and $b_{ij}$ coefficients | Acetone | Heptane | Toluene |
|---|---|---|---|
| $b_0$ | **0.0002*** | **<0.0001*** | **<0.0001*** |
| $b_1$ | **0.0091*** | **0.0411*** | 0.9261 |
| $b_2$ | **0.0034*** | **0.0023*** | **0.0007*** |
| $b_3$ | 0.2680 | 0.4466 | 0.1163 |
| $b_{11}$ | 0.0163 | 0.1245 | 0.1976 |
| $b_{22}$ | 0.6005 | 0.0520 | 0.3224 |
| $b_{33}$ | 0.7968 | 0.0838 | 0.7164 |
| $b_{12}$ | 0.1891 | 0.0634 | 0.8674 |
| $b_{13}$ | 0.6337 | 0.2645 | 0.1555 |
| $b_{23}$ | 0.5809 | 0.0806 | 0.4744 |

Note: *Significant factors.

### 3.2.1 Influence of the initial concentration $C_0$

Figure 6 represents the surface of response for the initial reaction rate $r_0$ versus light intensity $I$ and initial concentration $C_0$ for one of the targeted molecules, acetone.

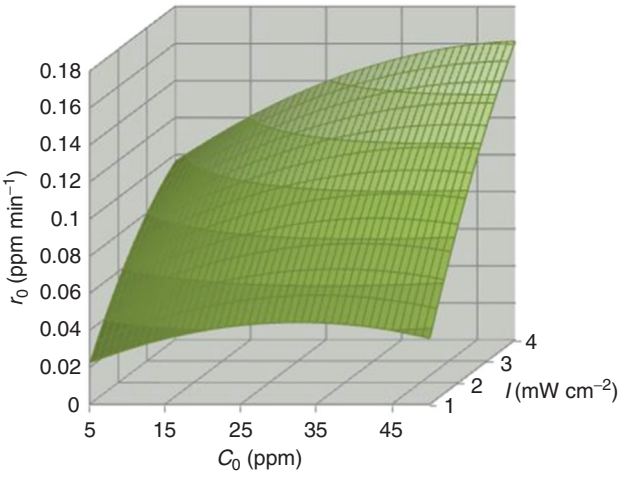


**Figure 6** Surface of response for the initial reaction rate $r_0$ versus light intensity $I$ and initial concentration $C_0$ for acetone

To analyse better the role of the initial concentration of pollutant on the initial reaction rate behaviour, a cross-section of the surface of response can be drawn for a fixed value of light intensity (Figure 7).

Looking at Figures 6 and 7, it can be observed that the initial concentration is influential regarding the initial reaction rate. The initial reaction rate $r_0$ increases with $C_0$ and reaches quite a steady value for $C_0$ higher than 35 ppmv or thereabouts. This general trend was observed for the three targeted molecules. The relationship between the reaction rate and the initial concentration is well known in heterogeneous photocatalysis. It is the starting point of the global kinetic model that was developed in this study, as described in the following part.

### 3.2.2 Influence of light intensity $I$

Numerous authors have already shown that light intensity is a significant parameter in the PCO of VOCs [9, 16]. Kim and Hong [9] proved that the reaction rate is related to the photon flux according to eq. (2):

$$r = k' I^n \tag{2}$$

where $r$ is the reaction rate (ppm min$^{-1}$), $k'$ is the kinetic constant (ppm min$^{-1}$ mW$^{-n}$ cm$^{2n}$) and $I$ is the light

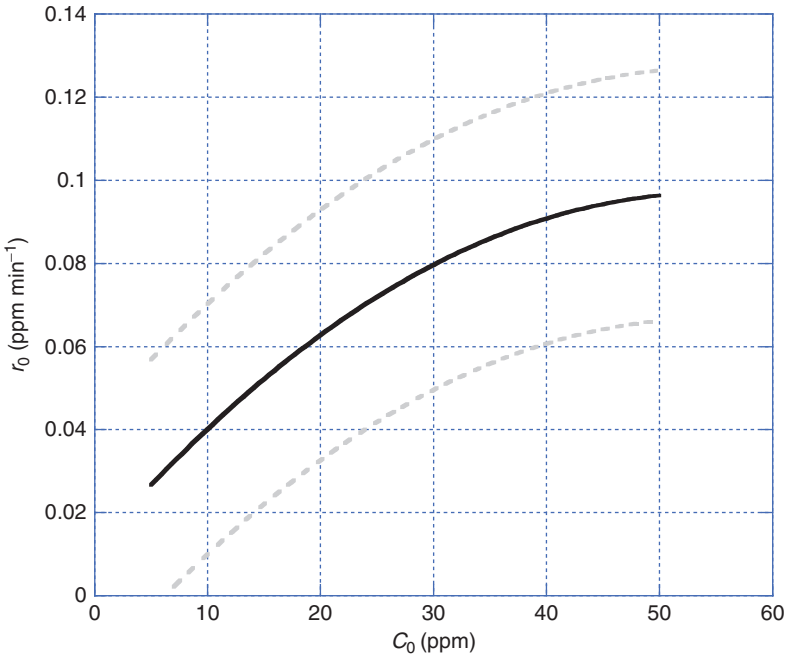


**Figure 7** Cross-section of the initial reaction rate $r_0$ versus initial concentration $C_0$ for acetone ($I = 2.5$ mW cm$^{-2}$ and $v = 0.6$ m s$^{-1}$)

intensity (mW cm$^{-2}$). The $n$ exponent generally takes values between 0 and 1. Actually, according to Herrmann [17], the influence of light intensity on the reaction rate may be divided into three different regimes: (1) first order where the electron/hole pairs are consumed more rapidly by the chemical reaction than by the recombination phenomenon, (2) 0.5 order where the recombination rate is predominant and (3) 0 order. Modestov and Lev [18] also found a change of $n$ from 1 to 0.5 over a certain level of photonic flux and explained it by an excess of photogenerated species ($e^-$, $h^+$ and $OH^\circ$).

In this study, we also tried to assess the influence of the light intensity regime. The order was determined by plotting the logarithm of the initial rate versus the logarithm of the light intensity under several operating conditions (Figure 8).

The order $n$ took values between 0.59 and 0.69, that is to say very close to 0.5. Consequently, it can be considered that, in the conditions of the present work, the regime driven by the light intensity is principally governed by a recombination phenomenon under UVA.

### 3.2.3 Influence of the upstream velocity *v*

Figure 9 shows the upstream velocity influence on the initial reaction rate for one given initial concentration of toluene. This influence is slightly negative with increasing velocity.

The upstream velocity in a dynamic reactor may have antagonist influences. In such a dynamic system, an increase in the upstream velocity improves the mass transfer but also decreases the contact time between the pollutant to be degraded and the photocatalytic medium. For instance, some authors have observed a reduction in conversion yield when the velocity is raised resulting from an insufficient contact time for flow rates between 0.02 and 1 m$^3$ h$^{-1}$ [19, 20]. Quici et al. [21], Zhong et al. [4] and Destaillats et al. [1] have also shown that a higher air recirculation rate does not lead to improved PCO air cleaning efficiency. On the contrary, other authors have noticed a positive effect of the increase in velocity (0.006–0.036 m$^3$ h$^{-1}$ for a cross-section of 78.5 cm$^2$) due to improving the mass transfer [22].

Mass transfer is a significant parameter that must be taken into account while conserving a dynamic regime. The Reynolds number is a good indicator to set the most appropriate regime. Obee demonstrated that for a Reynolds number over 500, the oxidation rate of toluene in a glass-plate reactor is less influenced by mass transfer [23].

In the present work, the Reynolds number is over 1,200 leading to a probably low mass transfer limitation. Consequently, contact time is more significant than mass transfer. As the reaction is performed in a multi-pass

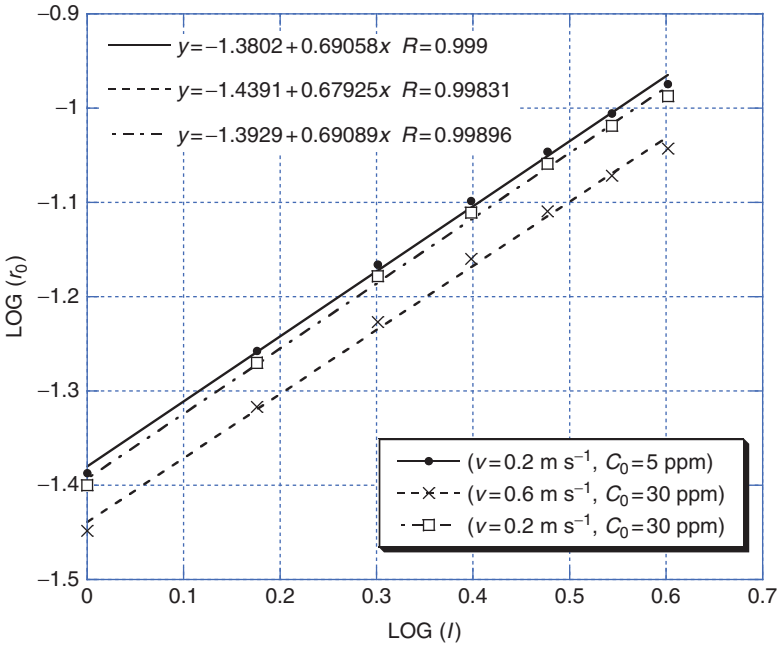


**Figure 8** Determination of the order of the power relation between $r_0$ and light intensity $I$ for toluene under UVA and three different operating conditions

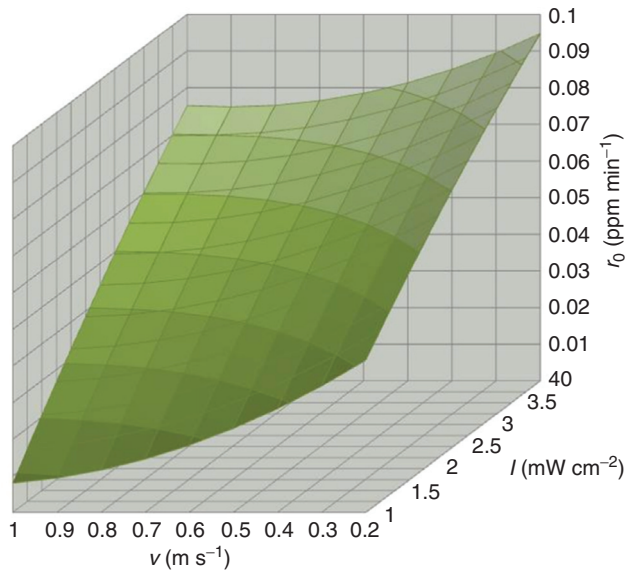


**Figure 9** Surface of response for the initial reaction rate $r_0$ versus the upstream velocity $v$ and the light intensity $I$ for toluene ($C_0$ = 27.5 ppm)

photocatalytic reactor, the contact time is directly related to the irradiation time. Thus, even if increasing the velocity has a negative influence, its impact on the oxidation rate is quite low.

## 3.3 A reaction mechanism approach and synthesizing a kinetic rate law

This part deals with the development of a simplified reaction mechanism and a rate law consistent with experimental observations and based on several hypotheses that are listed below:

1. In the range of concentrations studied, it is accepted that adsorption of VOC onto the photocatalytic medium involves only one type of adsorption site [2], i.e. Langmuir-type adsorption [14].
2. Oxygen is in excess in comparison with other reactants.
3. Adsorption of carbon dioxide onto the photocatalyst is negligible [24].
4. Adsorption of water vapour onto the photocatalytic medium is not taken into account in order to minimize the complexity of the problem.
5. The surface reaction is rate-controlling [25].
6. The reaction is carried out at steady state.
7. For VOC initial concentrations lower than 10 ppm, reaction intermediates are neglected.

Following these hypotheses, it is possible to write a simple mechanism for the photocatalytic degradation of

VOC considering only the steps of adsorption, surface reaction and desorption. Eqs (3)–(5) represent the proposed mechanism.

$$R + S \rightleftharpoons R \cdot S \text{ adsorption of VOC on the surface} \quad (3)$$

$$R \cdot S \rightarrow P \cdot S \text{ irreversible surface reaction to form products} \quad (4)$$

$$P \cdot S \rightleftharpoons P + S \text{ desorption of products from the surface} \quad (5)$$

Thus, each step is treated as an elementary reaction for writing the rate laws ($r_{AD}$ for adsorption, $r_S$ for surface reaction and $r_D$ for desorption). As surface reaction is rate-limiting, the global reaction rate law is equal to the surface reaction rate law (eq. (6)).

$$r'_R = r_S = k_S C_{R \cdot S} \quad (6)$$

where $k_S$ is the surface reaction rate constant and $C_{R\cdot\ S}$ is the surface concentration of sites occupied by $R$. Since the concentrations of adsorbed species cannot be readily measured, adsorption and desorption steps are used to express $C_{R\cdot\ S}$ versus measurable variables. By expressing the total concentration of sites $C_t$ at the catalyst surface and considering that the formed intermediates and by-products ($P$) can be neglected in this study, the global reaction rate law is written according to eq. (7).

$$r'_R = \frac{k_g K_A C_R}{1 + K_A C_R} \quad (7)$$

where $k_g = k_S C_t$ is the global reaction rate constant.

$K_A$ and $k_g$ are the two constants of the reaction rate law that have to be expressed as a function of the operating parameters using the DOE.

## 3.4 Determination of the model constants from the DOE

The objective of this paragraph is not only to calculate the values of $K_A$ and $k_g$ for the three studied VOCs but also to establish relationships between these constants and two operating parameters (light intensity $I$ and upstream air velocity $v$) as expressed by eq. (8).

$$r'_R = -\frac{dC_R}{dt} = \frac{k_g(I,v) K_A(I,v) C_R}{1 + K_A(I,v) C_R} \quad (8)$$

This equation can be integrated between the initial time of the reaction $t_0$ and a later time $t_0 + \Delta t$ (eq. 9).

$$\frac{\ln\left(\frac{C_{t_0}}{C_{t_0+\Delta t}}\right)}{\left(C_{t_0} - C_{t_0+\Delta t}\right)} = \frac{k_g K_A \Delta t}{\left(C_{t_0} - C_{t_0+\Delta t}\right)} - K_A \quad (9)$$

Because of the second chosen response variable ($y$ = conversion rate after 60 min of reaction) for the analysis of the DOE, $\Delta t$ was fixed at 60 min. In this way, as the conversion rate at 60 min was statistically modelled thanks to the results of the DOE, it was easy to calculate the value of $C_{t_0+\Delta t}$ for any initial concentration between 5 and 50 ppm. To respect the hypothesis made about the reaction intermediates (neglected), the highest initial concentration considered was fixed at 10 ppm. For each calculation of the constants, four initial concentrations ranging from 5 to 10 ppm were considered. For nine couples ($I$, $v$) using an OFAT approach and for the three VOCs, the quantity $\ln(C_{t_0}/C_{t_0+\Delta t})/(C_{t_0} - C_{t_0+\Delta t})$was plotted versus $1/(C_{t_0} - C_{t_0+\Delta t})$. The linear curves obtained enabled the values of $k_g$ and $K_A$ for each of the nine couples of operating parameters to be determined graphically. For confidential reasons, it is not possible to give these values. However, it was observed that the kinetic constant $k_g$ was only a function of light intensity in a power law way. This result is in accordance with Wang et al. [22]. At the same time, the equilibrium constant $K_A$ was found to be dependent on air velocity in a linear way but only for acetone. For toluene and heptane, no relationships were obtained between $K_A$ and $v$. Due to these observations, the reaction rate law could be finally written as follows:

$$r'_R = \frac{(a_m I^{b_m})(c_m + d_m v) C_R}{1 + (c_m + d_m v) C_R} \quad (10)$$

where $a_m$, $b_m$, $c_m$ and $d_m$ are constants that can be calculated from the results obtained from the DOE for each VOC.

## 3.5 Model validation and confirmation

The methodology described in the above paragraphs enabled a reaction kinetic model to be established in which the influence of the main identified parameters (light intensity $I$, upstream air velocity $v$ and VOC concentration $C$) is included. The last step of this methodology concerns the comparison of the experimental results with the model. Figures 10 and 11 hereafter illustrate this point for various concentrations of acetone and also different $I$ and $v$ values (Figure 10) and for identical operating conditions for the three studied VOCs (Figure 11). In these figures, dimensionless variables are considered with $t^*$ being equal to the half-degradation time.

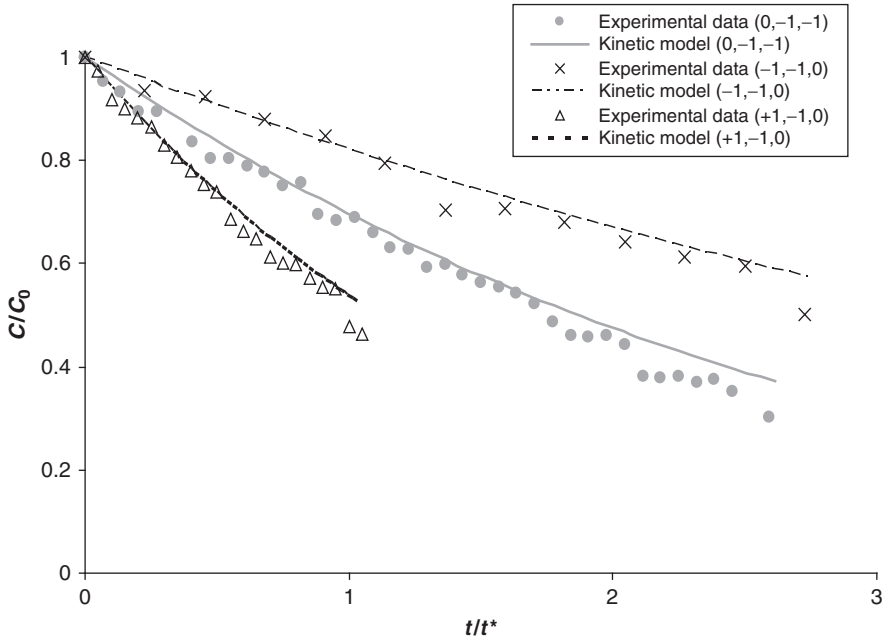


**Figure 10** Validation of the model for acetone (three different operating conditions)

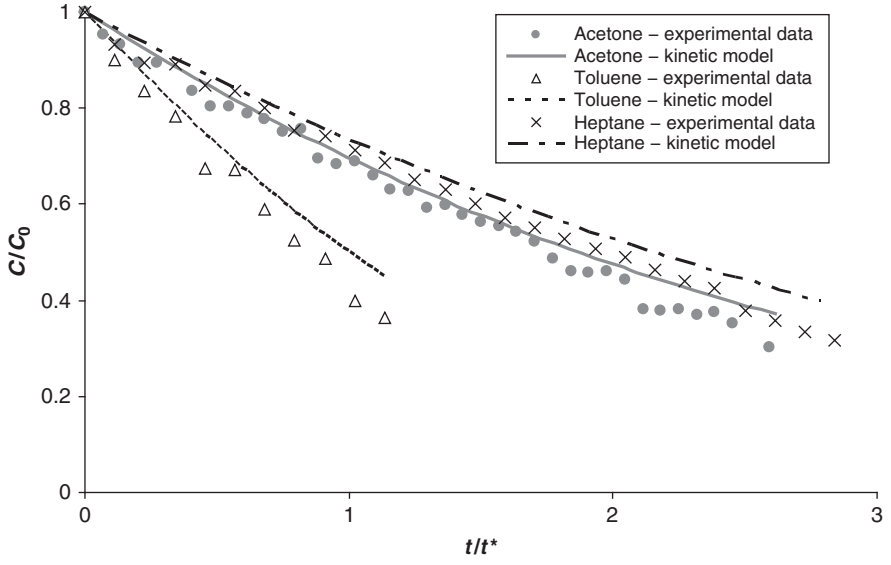


**Figure 11** Validation of the model for acetone, toluene and heptane in the same operating conditions ($I = 2.5$ mW cm$^{-2}$, $C_0 = 5$ ppm and $v = 0.2$ m s$^{-1}$)

According to Figures 10 and 11, it appears that the kinetic model fits the experimental data properly. The model is validated for the entire tested range of light intensity. Some complementary trials were also conducted for experiments not defined in the design matrix (Table 1), that is to say for light intensity and upstream air velocity not equal to the values coded –1, 0 and +1 but still in the studied ranges. These tests were also conclusive as the kinetic model was well in accordance with the experimental results during the first 60 min of reaction. Over that reaction time, the kinetic model tended to overestimate the degradation time slightly with the model curve being just above the experimental points.

## 4 Conclusions

An original and economical methodology using BBDs of experiments was implemented to study the photocatalytic degradation of three common indoor VOCs. A predictive model based on a reaction mechanism approach and a kinetic rate law including certain operating parameters was built. It was shown that the model fits properly the experimental curves in the range of concentration, light intensity and air flow studied. This methodology can be used for any other photocatalysts and for VOC initial concentrations closer to indoor environment values.

## References


1. Destaillats H, Sleiman M, Sullivan DP, Jacquiod C, Sablayrolles J, Molins L. Key parameters influencing the performance of photocatalytic oxidation (PCO) air purification under realistic indoor conditions. Appl Catal B: Environ 2012;128:159–70.
2. Pichat P. Some views about indoor air photocatalytic treatment using $TiO_2$: conceptualization of humidity effects, active oxygen species, problem of $C_1$–$C_3$ carbonyl pollutants. Appl Catal B: Environ 2010;99:428–34.
3. Zhao J, Yang X. Photocatalytic oxidation for indoor air purification: a literature review. Build Environ 2003;38:645–54.
4. Zhong L, Haghighat F, Blondeau P, Kozinski J. Modeling and physical interpretation of photocatalytic oxidation efficiency in indoor air applications. Build Environ 2010;45:2689–97.
5. Mo JH, Zhang YP, Xu QJ, Lamson JJ, Zhao R. Photocatalytic purification of volatile organic compounds in indoor air: a literature review. Atmos Environ 2009;43:2229–46.
6. Sakkas VA, Islam MA, Stalikas C, Albanis TA. Photocatalytic degradation using design of experiments: a review and example of the Congo red degradation. J Hazard Mater 2010;175:33–44.
7. Herrmann J-M. Heterogeneous photocatalysis: an emerging discipline involving multiphase systems. Catal Today 1995;24:157–64.
8. Kirchner S, Arenes JF, Cochet C, Derbez M, Duboudin C, Elias P, et al. 2006. Campagne nationale logements. Etat de la qualité de l'air dans les logements français. Observatoire de la Qualité de l'Air Intérieur, Rapport final (in French).
9. Kim S, Hong S. Kinetic study for photocatalytic degradation of volatile organic compounds in air using thin film $TiO_2$ photocatalyst. Appl Catal B: Environ 2002;35:305–15.
10. Raillard C, Héquet V, Le Cloirec P, Legrand J. $TiO_2$ coating types influencing the role of water vapor on the photocatalytic oxidation of methyl ethyl ketone in the gas phase. Appl Catal B: Environ 2005;59:213–20.
11. Mohseni M, David A. Gas phase vinyl chloride (VC) oxidation using $TiO_2$-based photocatalysis. Appl Catal B: Environ 2003;46:219–28.
12. Shie J-L, Lee C-H, Chiou C-S, Chang C-T, Chang C-C, Chang C-Y. Photodegradation kinetics of formaldehyde using light sources of UVA, UVC and UVLED in the presence of composed silver titanium oxide photocatalyst. J Hazard Mater 2008;155:164–72.
13. Maudhuit A, Raillard C, Héquet V, Le Coq L, Sablayrolles J, Molins L. Indoor air purification. Photocatalytic process for the removal of toluene. In: Department of Sanitary and Environmental Engineering, Kassel Universität, editor. Odours and VOCs: measurement, regulation and control techniques. Kassel, 2010:295–303.
14. Maudhuit A, Raillard C, Héquet V, Le Coq L, Sablayrolles J, Molins L. Adsorption phenomena in photocatalytic reaction: the case of acetone, toluene and heptane. Chem Eng J 2011;170:464–70.
15. Ferreira SL, Bruns RE, Ferreira HS, Matos GD, David JM, Brandão GC, et al. Box–Behnken design: an alternative for the optimization of analytical methods. Anal Chim Acta 2007;597:179–86.
16. Jeong J, Sekiguchi K, Sakamoto K. Photochemical and photocatalytic degradation of gaseous toluene using short-wavelength UV irradiation with $TiO_2$ catalyst: comparison of three UV sources. Chemosphere 2004;57:663–71.
17. Herrmann J-M. Heterogeneous photocatalysis: state of the art and present applications. Top Catal 2005;34:49–65.
18. Modestov A, Lev O. Photocatalytic oxidation of 2,4-dichlorophenoxyacetic acid with titania photocatalyst. Comparison of supported and suspended $TiO_2$. J Photochem Photobiol A 1998;112:261–70.
19. Biard P-F, Bouzaza A, Wolbert D. Photocatalytic oxidation of two volatile fatty acids in monocomponent and multicomponent systems: comparison between batch and annular photoreactors. Appl Catal B: Environ 2007;74:187–96.
20. Sleiman M, Conchon P, Ferronato C, Chovelon J-M. Photocatalytic oxidation of toluene at air levels (ppbv): towards a better assessment of conversion, reaction intermediates and mineralization. Appl Catal B: Environ 2009;86:159–65.
21. Quici N, Vera ML, Choi H, Li Puma G, Dionysiou DD, Litter MI, et al. Effect of key parameters on the photocatalytic oxidation of toluene at low concentrations in air under $254 + 185$ nm UV irradiation. Appl Catal B: Environ 2010;95:312–19.
22. Wang K-H, Tsai H-H, Hsieh Y-H. The kinetics of photocatalytic degradation of trichloroethylene in gas phase over $TiO_2$ supported on glass bead. Appl Catal B: Environ 1998;17:313–20.
23. Obee T. Photooxidation of sub-parts-per-million toluene and formaldehyde levels on titania using a glass-plate reactor. Environ Sci Technol 1996;30:3578–84.
24. Sauer M, Ollis D. Acetone oxidation in a photocatalytic monolith reactor. J Catal 1994;149:81–91.
25. Fogler HS. Elements of chemical reaction engineering, 2nd ed. Upper Saddle River, NJ: Prentice Hall International Editions, 1992.